The Ftr1p iron permease in the yeast plasma membrane: orientation, topology and structure–function relationships

Scott SEVERANCE, Satadipta CHAKRABORTY and Daniel J. KOSMAN[1]

Department of Biochemistry, School of Medicine and Biomedical Sciences, State University of New York at Buffalo, Buffalo, NY 14214, U.S.A.

Ftr1p is the permease component of the Fet3p–Ftr1p high affinity iron-uptake complex, in the plasma membrane of *Saccharomyces cerevisiae*, that transports the Fe^{3+} produced by the Fet3p ferroxidase into the cell. In this study we show that Ftr1p probably has seven transmembrane domains with an orientation of N-terminal outside, and C-terminal inside the cell. Within the context of this topology of the Fet3p–Ftr1p complex, we have identified several sequence elements in Ftr1p that are required for wild-type uptake function. First to be identified were two REXLE (Arg-Glu-Xaa-Leu-Glu) motifs in transmembrane domains 1 and 4. Alanine substitutions at any one of these combined six arginine or glutamic acid residues inactivated Ftr1p in iron uptake, indicating that both motifs were essential to iron permeation. R → K and E → D substitutions in these two motifs led to a variable loss of activity, suggesting that while all six residues were essential, their contributions to uptake were quantitatively and/or mechanistically distinct. The terminal glutamate in an EDLWE[89] element, associated with transmembrane domain 3, and a DASE motif, located in extracellular loop 6, were also required. The double substitution to AASA in the latter, inactivated Ftr1p in iron uptake while the Ftr1p(E89A) mutant had only 20 % of wild-type activity. The two REXLE and the EDLWE and DASE motifs are strongly conserved among fungal Ftr1p homologues, suggesting that these motifs are essential to iron permeation. Finally another important residue, Ile^{369}, was identified in the Ftr1p cytoplasmic C-terminal domain. Deletion or substitution of this residue led to a 70 % loss of iron-uptake activity. Ile^{369} was the only residue identified in this domain that made such a major contribution to iron uptake by the Fet3p–Ftr1p complex.

Key words: Ftr1 protein, iron trafficking, iron transport, yeast iron permease.

INTRODUCTION

The most commonly studied fungi include the yeasts *Saccharomyces cerevisiae*, *Schizosaccharomyces pombe* and *Candida albicans*. The genomes of all three organisms encode a pair of proteins that, in each strain, have been genetically and biochemically linked to high-affinity iron uptake. First identified and characterized in *S. cerevisiae*, these are the Fet3p and Ftr1p proteins [1–10].

The proximal substrate for high-affinity iron uptake mediated by Fet3p/Ftr1p is the ferrous ion, Fe^{2+}. Whether present as a result of a reducing environment, or produced from Fe^{3+} by the action of a plasma membrane metalloreductase(s) that is also produced by these and most other eukaryotes [6–8,11,12], this Fe^{2+} is oxidized (or re-oxidized) into the ferric ion, Fe^{3+}. This first step in the yeast high-affinity iron-uptake pathway, in which O_2 is reduced by $4Fe^{2+}$ to $2H_2O$, is an example of what is called the 'ferroxidase' reaction [7,11,13]. This reaction is catalysed by Fet3p (and its orthologues), which is a member of the multicopper oxidase class of copper proteins [1,3,5,7]. In *S. cerevisiae* the Fe^{3+} produced by the Fet3p-catalysed ferroxidase reaction is the substrate for the iron permease, Ftr1p [10].

Genetic and biochemical data suggest that Fet3p/Ftr1p form, or are part of, a (protein) complex in the yeast plasma membrane [10,14,15]. The basic fact in this regard is that trafficking of either protein to the plasma membrane requires the co-trafficking of the other. For example, an Ftr1p–YFP (yellow fluorescent protein) fusion protein remains intracellular when produced in an *fet3Δ*-containing background. In contrast, this fluorescent fusion protein is clearly seen localized to the plasma membrane when the host strain is co-transformed with a *FET3*-containing plasmid [14]. Also, in the absence of Ftr1p, any Fet3p produced remains in a vesicular compartment within the cytoplasm [10,15]. Although there are no published data that directly demonstrate an interaction between Fet3p and Ftr1p, co-immunoprecipitation results have shown that the vacuole-localized homologous pair, the Fet5p and Fth1p paralogues in *S. cerevisiae*, do interact [16]. Thus, that Fet3p/Ftr1p are in close proximity is strongly inferred even if the precise nature of this putative complex has not been characterized.

Fet3p is a type I membrane protein with a single transmembrane domain found close to the protein's C-terminus, which is oriented to the inside of the cell. The multicopper oxidase domain, which comprises the major part of the protein, is oriented outside [3,5,7]; the orientation and topology of Ftr1p have not been established. A first model suggested that it had six transmembrane domains with both the N- and C-termini outside [10]. On the other hand, as briefly discussed here, most algorithms predict that Ftr1p has seven membrane-spanning helices, with an overall orientation of N-terminal out, C-terminal in. Based on results shown here, these predictions are probably correct. The most important single fact about the pathway of iron uptake through the Fet3p/Ftr1p pair is that Fe^{3+} itself is not a substrate for iron permeation through Ftr1p. Iron taken into the cell through Ftr1p must 'come' from the ferroxidation reaction catalysed by Fet3p [7]. This obligatory epistatic relationship suggests a model in which iron 'enters' this iron-uptake pathway through Fet3p, which then hands its product Fe^{3+} off to Ftr1p for permeation. This is a classic description of substrate channelling [17], and is equivalent to the concept and

Abbreviations used: (yE)GFP, (yeast-enhanced) green fluorescent protein; E185A etc., substitution of Glu^{185} with alanine etc.; FRET, fluorescence resonance energy transfer; HA, haemagglutinin; ORF, open reading frame; R → K etc., substitution of an arginine residue with lysine etc. (single-letter amino acid coding); REXLE motif etc., amino acid motifs and sequences use the single-letter amino acid coding; TM, transmembrane; YFP, yellow fluorescent protein.

[1] To whom correspondence should be addressed (e-mail camkos@buffalo.edu).

role of the metal chaperones that are so well-studied in eukaryotic copper metabolism [18,19].

This model of iron channelling in the putative Fet3p/Ftr1p complex requires that there are amino acid residues in each protein that contribute to this trafficking process. In addition to these residues, there should also be some that contribute to the initial binding of Fe^{2+} to Fet3p, and to the ferroxidation reaction, and those in Ftr1p that contribute to the permeation process itself. Three iron-binding residues on Fet3p have been identified by kinetic analyses of the ferroxidation reaction catalysed by site-specific proteins *in vitro*. One of these residues, Glu^{185}, also contributes to steps subsequent to the ferroxidation reaction, perhaps to the trafficking of Fe^{3+} to Ftr1p. This is indicated by the ferroxidase positive, uptake negative phenotype of a Fet3p(E185A) mutant (where E185A is the substitution of Glu^{185} with alanine) [14].

The objective of this study was to identify residues on Ftr1p that contribute similarly to steps in uptake that occur subsequent to ferroxidation. To assign objectively this function to any residue, we first experimentally confirmed the predicted orientation and topology of Ftr1p. We then investigated the trafficking and iron-uptake function of insertion and truncation mutants. Lastly we targeted specific residues for substitution so as to assess the contribution that several sequence motifs make to iron trafficking by Ftr1p.

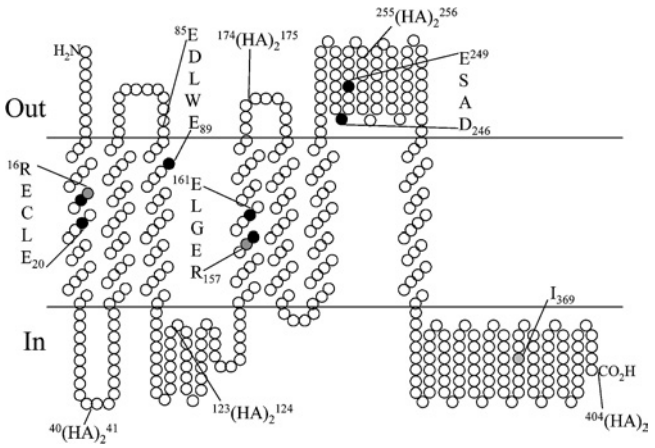

Figure 1 Topological model of Ftr1p in the yeast plasma membrane

This model was generated at SOSUI (http://sosui.proteome.bio.tuat.ac.jp/sosuiframe0.html). The five $(HA)_2$ insertions used to test this model by indirect immunofluorescence are indicated, as are the five sequence elements identified herein as required for wild-type iron-uptake activity. These are: REXLE motifs in transmembrane domains 1 and 4; a DASE motif in extracellular loop 6; E^{89} in the ^{85}EDLWE^{89} element adjacent to TM3; and I^{369} in the cytoplasmic C-terminal domain. Note that Fet3p, the ferroxidase that assembles with Ftr1p to support high affinity in *S. cerevisiae*, has a single transmembrane domain that places this enzyme's oxidase active site at the extracellular surface of the yeast plasma membrane.

EXPERIMENTAL

Strains, media and culture conditions

Isogenic strains DEY1457 (*MATα can1 his3 leu2 trp1 ura3 ade6*); 1457*ftr1Δ* (DEY1457 *ftr1::TRP1*); and 1457*fet3Δftr1Δ* (DEY1457 *fet3::HIS3 ftr1::TRP1*) were used in the indirect immunofluorescence and *in situ* confocal fluorescence co-localization studies. The parental strains, DEY1457 and DEY1394 (DEY1457 *fet3::HIS3*), were provided by Dr D. Eide (University of Missouri, Columbia, MO, U.S.A.) [20]. Strain 1457*ftr1Δfet4Δ* (DEY1457 *ftr1::TRP1 fet4::kanMX4*) was used as a negative control in iron-uptake analysis of the activity of all modified forms of Ftr1p. This strain, which has no saturable iron-uptake activity, was constructed by serial backcrossing progeny of 1457*ftr1Δ* × YO6461 with 1457*ftr1Δ*. YO6461 (*MAT*a *his3 leu2 met15 ura3 fet4::kanMX4*) was obtained from Open Biosystems (Huntsville, AL, U.S.A.). Overnight cultures were grown in selective media (6.67 g/l yeast nitrogen base without amino acids, 2 % glucose plus the appropriate drop-out mixture of amino acids), and then used as inocula into media containing 500 μM ferrozine to induce the iron deficiency requisite to the expression of *FET3* and *FTR1*. Early log-phase cells ($D_{660} = 0.8$–2.0) were used for all experiments.

Plasmid constructions

All plasmids containing the *FTR1* coding sequence were based on plasmid p703FTR1. This vector is pRS415 containing the 2.2 kb *FTR1* transcription unit [10]. Site-directed mutant *FTR1* sequences were generated in one step using the QuikChange kit from Stratagene (La Jolla, CA, U.S.A.) and the appropriate primer pair. Using either p703FTR1 or a p703FTR1 plasmid containing a previously constructed truncation as template, C-terminal truncations were prepared similarly by a 'looping out' approach. Half of each primer annealed immediately 3′ of the *FTR1* ORF (open reading frame). The other half of each primer annealed to the 15–20 bases 5′ to, and including, the bases encoding the amino acid residue at the C-terminal of the new truncation protein. p703FTR1–YFP was constructed in two steps [14]. First, the YFP coding sequence was amplified from plasmid pDH5 obtained from the Yeast Resource Center, University of Washington (Seattle, WA, U.S.A.). This PCR product was then used as a megaprimer to 'loop-in' YFP encoding sequences into the 3′ end of the *FTR1* gene in p703FTR1 using the QuikChange protocol. pDY134, based on pRS416, contains the *FET3* transcription unit [14]. This vector was slightly modified so that the yEGFP (yeast-enhanced green fluorescent protein) encoding sequence could be ligated to the 3′ end of *FET3*. Both pRS415 and pRS416 are centromere-based, low copy plasmids in yeast [21]. The yEGFP reading frame was from pUG34, a gift from Dr Hans Hegemann, University of Dusseldorf, Dusseldorf, Germany (see also [22]).

Insertion of the double haemagglutinin $(HA)_2$ epitope, used in indirect immunofluorescence studies, was accomplished by PCR using two pairs of primers and with p703FTR1 as template. In each primer pair, one primer amplified from the end of the *FTR1* transcription unit and the other primer (containing a *Not*I site and encoding an HA tag) amplified from the Ftr1p residue position at which the $(HA)_2$ tag was to be inserted. The reaction amplifying the 5′ end of the transcription unit yielded a product with unique *Bam*HI and *Not*I sites at opposite ends. The reaction amplifying the 3′ end of the transcription unit yielded a product with unique *Sac*I and *Not*I sites at opposite ends. After digesting the *FTR1* 5′ PCR product with *Bam*HI and *Not*I, the *FTR1* 3′ PCR product with *Sac*I and *Not*I, and pRS415 with *Bam*HI and *Sac*I, a three-way ligation was performed to obtain the desired product. All constructs were confirmed by automated fluorescent sequencing on an ABI PRISM 377 instrument.

Indirect immunofluorescence

Strain 1457*ftr1Δ* was freshly transformed with plasmid p703FTR1 that contained the encoded Ftr1p–$(HA)_2$ fusions as shown in Figure 1. Transformants were grown as described above; after approx. 4 h of growth in the presence of 500 μM ferrozine, paraformaldehyde (37 %) was added to a final concentration of 3.7 % (v/v). The fixed cells were pelleted by centrifugation at

3000 ***g*** for 2 min at 4 °C, washed twice with 100 mM potassium phosphate buffer, pH 6.5, washed once with the same buffer containing 1.2 M sorbitol, and resuspended in 2 ml of this sorbitol buffer. The cells were spheroplasted at 37 °C following addition of 2 μl of 1.0 M dithiothreitol, 10 μl 2-mercaptoethanol, and 20 μl 10 mg/ml Zymolyase 20T (Seikagaku, Tokyo, Japan). The fixed spheroplasts (40 μl) were plated on poly-lysine-coated coverslips which were then rinsed four times with 1 ml of the sorbitol buffer. Half of the coverslips were kept in this buffer, while the fixed spheroplasts on the other half were permeabilized by treatment with PBS, pH 7.3, containing 0.4 % Triton X-100 for 2 min. All samples were subsequently blocked with PBS containing 1.0 % BSA (w/v, Sigma) followed by incubation for 1 h with primary antibody [HA-probe (F-7) sc-7392; Santa Cruz Biotechnology, Santa Cruz, CA, U.S.A.]. After removal of the primary antibody solution, coverslips were then incubated for 1 h with secondary antibody [Cy™5-conjugated AffiniPure Rabbit Anti-Mouse IgG (H + L); Jackson ImmunoResearch Laboratories, West Grove, PA, U.S.A.]. The secondary antibody solution was removed, and the cover slips were washed six times with PBS (0.1 % BSA). An anti-fade solution (11 μl, consisting of 20 mg of n-propylgallate dissolved in 8 parts glycerol and 2 parts PBS, pH 7.3) was placed in each well of two-well printed microscope slides (PGC Scientifics, Gaithersburg, MD, U.S.A.). A coverslip was placed on top of the anti-fade solution and sealed with VALAP (1:1:1 by vol. mixture of vaseline, paraffin, and lanolin). Slides were kept at − 20 °C until 1 h before viewing, at which point they were allowed to reach room temperature.

Images of spheroplast (indirect immunofluoresence) or live cell (GFP and YFP fusions) fluorescence were obtained by confocal fluorescence microscopy using a BioRad MRC 1024 confocal system equipped with a 15 MW krypton/argon laser and operating on a Nikon Optiphot upright microscope and an oil immersion 60 × 1.4 NA objective. Optical sections were acquired at 0.5 μm and the XY resolution was set at $\geqslant$ 0.2 μm using BioRad's Lasersharp V3.0 software and later processed using Confocal Assistant V4.02 (available at ftp.genetics.bio-rad.com).

Fluorescence quantification of Ftr1p–YFP fusion proteins

Cells producing wild-type and mutant forms of Ftr1p–YFP were grown as above and then washed twice with 25 mM Tris, pH 6.8 (FRET buffer), and resuspended in 1 ml of FRET buffer [23]. Cell aliquots (2×10^7 cells) were diluted in this buffer to a total volume of 3 ml. Ftr1p–YFP production in these cells was determined by scanning fluorescence emission spectroscopy using a Perkin-Elmer Model LS50B luminescence spectrometer. For detection of YFP fluorescence, 510 nm excitation was used, and emission was recorded between 520 nm and 610 nm (slits set at 4.0 nm). The FL-Win Lab software, Firmware E5, was used to collect the emission spectra and then to correct these spectral envelopes for the auto-fluorescence of cells expressing the non-fluorescent Ftr1p control. The resulting difference spectral envelopes, which were the signal-averaged values from five scans, were quantified to yield the relative fluorescence of the several fluorophore-tagged protein species. For several of these species this quantification was the result of three independent analyses; for these, the data were statistically evaluated using Prism3 software (GraphPad, San Diego, CA, U.S.A.).

Iron-uptake assays

Iron-uptake assays were performed as decribed previously [24]. Briefly, cells (grown as decribed above) were washed and resuspended in uptake buffer [Mes, pH 6.0, containing 2 % (w/v) glucose and 20 mM citrate]. Cells (2×10^7 per ml of uptake buffer) were added to uptake buffer containing 20 mM ascorbate and incubated, with shaking, for 15 min. ^{59}Fe (to 0.2 μM) was added to initiate the uptake reaction. Samples (1 ml) were quenched in 3 ml of an ice-cold solution of 0.1 M Tris succinate, pH 6.0, containing 1 mM EDTA and then washed four times with this quench buffer. Samples were counted on a Wallac model 1480 Wizard gamma counter with correction made for non-specific cell accumulation of ^{59}Fe using the uptake values measured for the parental 1457*ftr1*Δ strain. The uptake values given are taken from a linear uptake range, 1–10 min. All values are means from at least three independent experiments done in triplicate. Statistical analysis of these data was performed using the Prism3 software.

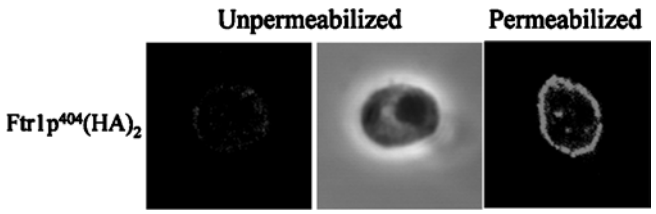

Figure 2 Cytoplasmic C-terminus of Ftr1p is revealed by indirect immunofluoresence

Fixed spheroplasts prepared from yeast strain 1457*ftr1*Δ producing Ftr1p–^{404}(HA)$_2$ (C-terminal tag) from a low copy number plasmid under control of the *FTR1* promoter, were probed with anti-HA antibody either without or with prior permeabilization as indicated. The left- and right-hand panels are confocal images while the central panel is a phase-contrast image of the unpermeabilized sample.

RESULTS

Orientation and topology of Ftr1p in the yeast plasma membrane

By experiment and comparison with known structures, Heijnea and co-workers [25,26] demonstrated that membrane topology can be predicted with > 90 % confidence by the use of multiple topology algorithms and the resulting 'majority vote'. Of the seven such algorithms that we employed to predict the topology of Ftr1p (TMHMM, HMMTOP, TOPPREDII, PHD, SOSUI, DAS, and MEMSAT), six are designed to predict overall orientation (all except DAS). Five of these six programs predicted that the most likely orientation of Ftr1p in the yeast plasma membrane is N-terminal out. Five of the seven algorithms generated a 'best' model that had seven TM (transmembrane domains; TMHMM, HMMTOP, PHD, SOSUI, DAS). In summary, Ftr1p is predicted to be oriented N-terminal out, and with seven transmembrane domains, will have the C-terminus in the cytoplasm. A representation of this model, generated by SOSUI, is shown in Figure 1.

This model was tested directly by indirect immunofluorescence analyses based on a series of Ftr1p proteins tagged with the (HA)$_2$ epitope (noted in Figure 1). Thus to evaluate the orientation of the Ftr1p C-terminus, an Ftr1p–^{404}(HA)$_2$ fusion protein (C-terminal epitope tag) was produced from a low copy plasmid in an *ftr1*Δ-containing strain. The cell sample was fixed for indirect immunofluorescence analysis, the cell walls were removed, and the resulting spheroplasts divided into two aliquots. The first aliquot was probed directly with primary anti-HA antibody, and then with the fluorescently tagged secondary one. The second aliquot was first permeabilized with Triton X-100 and then probed with primary and secondary antibodies. These two samples were then examined by confocal fluorescence microscopy.

As illustrated in Figure 2, the C-terminal epitope in the fusion protein was probed by the primary antibody only in permeabilized cells; this epitope in the unpermeabilized cells was inaccessible.

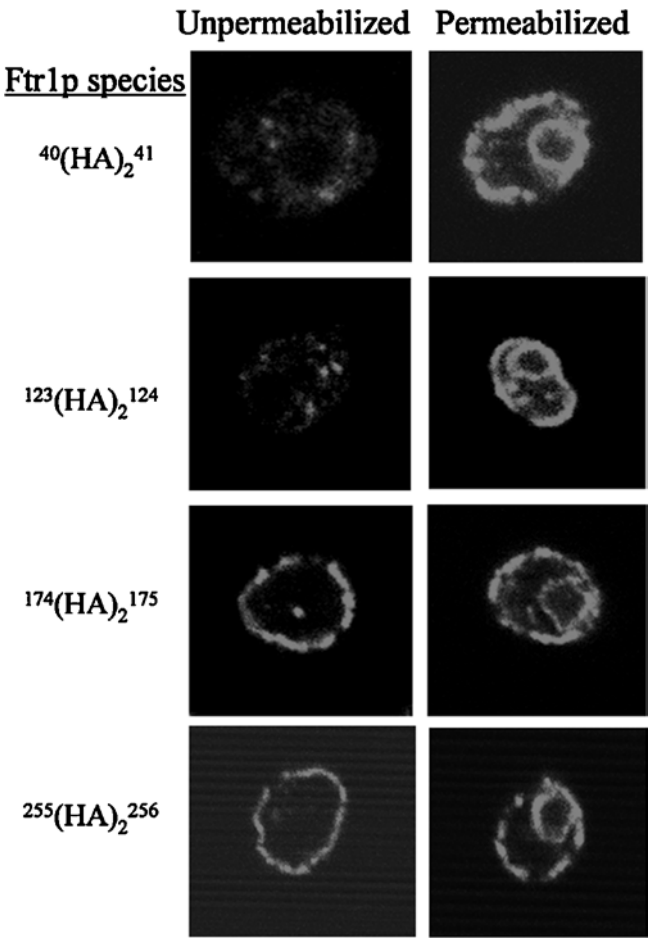

Figure 3 Ftr1p topology as revealed by indirect immunofluoresence

Fixed spheroplasts prepared from yeast strain 1457*ftr1Δ* producing the Ftr1p–$(HA)_2$ fusions indicated, were processed for indirect immunofluorescence as described in Figure 2. The accumulation of these fusions in the perinuclear space seen here was variable and probably due to a variable level of epitope-tagged protein production. This feature fortuitously provided an internal control of membrane integrity in the unpermeabilized samples, e.g. for Ftr1p–$^{174}(HA)_2{}^{175}$ and Ftr1p–$^{255}(HA)_2{}^{256}$.

A phase-contrast image of these latter cells is included to help in locating the cell in the fluorescence image on the left-hand side. This result indicates that the Ftr1p C-terminus is inside the cell, as predicted by the topology model.

To further test this model, the $(HA)_2$ epitope was inserted into the four largest of the six predicted loop regions in the overall Ftr1p conformational fold. These insertions were between residues 40/41, loop 1 (cytoplasmic); 123/124, loop 3 (cytoplasmic); 174/175, loop 4 (extracellular); and 255/256, loop 6 (extracellular); the orientations indicated in parentheses are those predicted as shown in Figure 1. All four epitope-tagged proteins were produced in the *ftr1Δ*-containing strain as above. The transformants were tested for iron-uptake activity to confirm the activity of these Ftr1p fusions, and the orientation of the epitope tag in each protein was determined by indirect immunofluorescence.

Fluorescence was observed localized to the plasma membrane in each cell sample producing one of the $(HA)_2$-tagged Ftr1p proteins. However, in the case of the 40/41 and 123/124 insertions (in predicted cytoplasmic loops), this fluorescent signal was seen only in permeabilized spheroplasts and not in the unpermeabilized sample (Figure 3). In contrast, fluorescence was observed from the 174/175 and 255/256 insertions (in predicted extracellular loops) in the unpermeabilized samples as well as the permeabilized ones. This pattern of immunofluorescence detection was fully consistent with the model illustrated in Figure 1. Note that the iron uptake measured in transformants producing any one of the five $(HA)_2$-tagged Ftr1p proteins ranged from 50–110 % of the uptake supported by episomally produced wild-type Ftr1p in the same 1457*ftr1Δ* strain (results not shown).

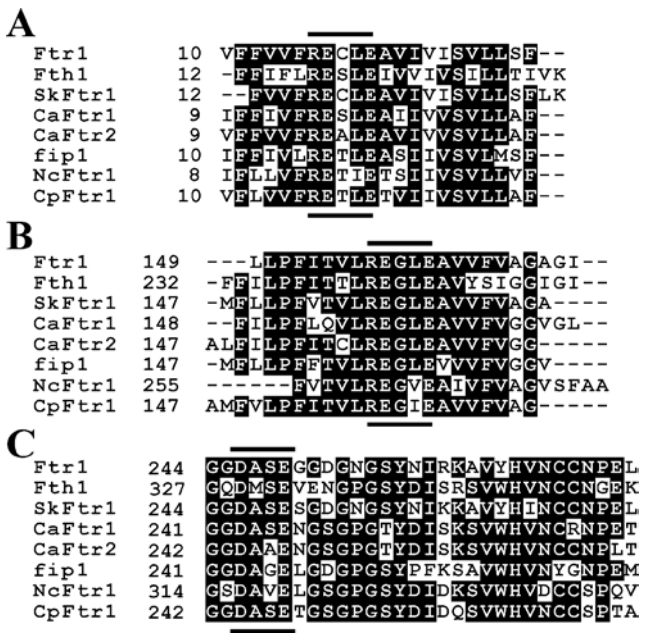

Figure 4 Functional motifs suggested by sequence alignments of fungal Ftr1p homologues

These alignments focus on predicted transmembrane domains 1 and 4 (panels **A** and **B** respectively) and extracellular loop 6 (panel **C**). The functional motifs in these three domains are underlined: RE(C/G)(L/V/I)E in TM1; REG(L/V/I)E in TM4; and D(A/M)(S/A/G/V)E in loop 6. Ftr1p and Fth1p are from *S. cerevisiae*; fip1 is from *Schizosacchromyces pombe*. Sk, *Saccharomyces kluyveri*; Ca, *Candida albicans*; Nc, *Neurospora crassa*; and Cp, *Claviceps purpurea*.

Functional motifs in Ftr1p by homology

Ftr1p and its homologues in *S. cerevisiae* and other yeasts and fungi contain multiple E/DXXE motifs [7]. One group of these motifs has the sequence REXZE, where X is most commonly glycine and Z is most commonly leucine. All Ftr1p homologues contain two of this type of motif, one in TM1 and the other in TM4. In Ftr1p these two motifs are ^{16}RECLE^{20} and ^{157}REGLE^{161} respectively (these sequences are indicated in the topology model in Figure 1). The alignments of these two motifs in some of the archived fungal Ftr1p homologues are shown in Figures 4(A) and 4(B) respectively.

Also, all Ftr1p homologues contain E, D or ED elements that are located near or at the interfaces between loop and membrane regions of the protein fold, or in the larger of the loop regions. The most conserved of these is ^{85}E(D/E)XXE^{89} that spans the predicted interface between loop 2 (extracellular) and TM3 and ^{246}DXXE^{249} in loop 6 (extracellular) and is the largest of the predicted loop regions in the topological map (residue numbers for ScFtr1p). Both of these elements are indicated in Figure 1. The alignment of the latter sequence in the fungal Ftr1p homologues is shown in Figure 4(C).

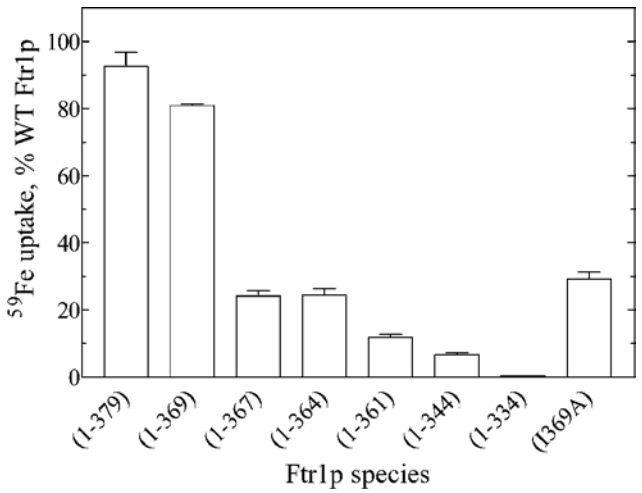

Figure 5 Probing the functional role of the Ftr1p C-terminal domain

Serial C-terminal truncations of Ftr1p were prepared in plasmid p703FTR1 by 'looping out' the sequence regions indicated in the Figure. Ftr1p(I369A) was constructed by site-directed mutagenesis using the QuikChange kit from Stratagene and the appropriate primer pair. Wild-type and mutant Ftr1p proteins were produced in strain 1457*ftr1Δ* under control of the wild-type *FTR1* promoter in the presence of 500 μM ferrozine. ^{59}Fe uptake analysis of these transformants was carried out in 0.1 M Mes, pH 6.0, with 0.2 μM ^{59}Fe (a concentration equal to the K_m^{Fe} [12]) in the presence of 20 mM each of citrate and ascorbate. Uptake values were corrected for non-specific ^{59}Fe binding (uptake at $t = 10$ s) and for ^{59}Fe uptake in the uptake-negative 1457*fet4Δftr1Δ* strain ($\leqslant$ 0.1 pmol ^{59}Fe/10^7 cells/10 min). The values are given as a percent of the uptake value (mean $\pm$ S.E.) for the wild-type Ftr1p transformant which was 14.8 $\pm$ 0.6 pmol ^{59}Fe/10^7 cells per 10 min.

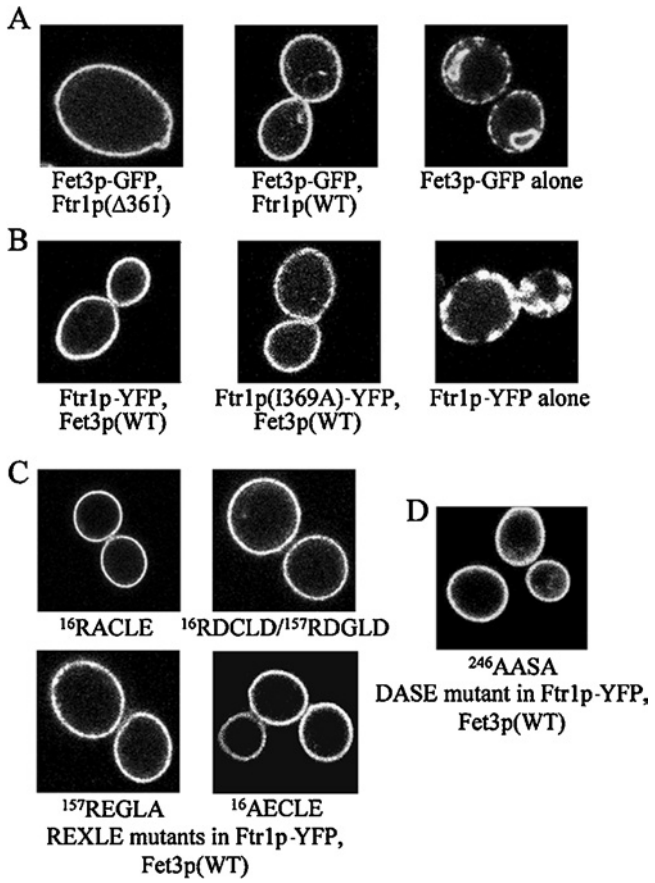

Figure 6 Wild-type plasma membrane localization of Ftr1p mutants

Ftr1p–Fet3p species in the cells pictured in these confocal, fluorescent images are given for each sample. (**A**) Strain 1457*fet3Δftr1Δ* was transformed with p134FET3–GFP and p703FTR1(Δ361) (left-hand image); or p134FET3–GFP and p703FTR1(wild-type) (middle image); or with p134FET3–GFP alone (right-hand image). The equivalent plasma membrane localization of Fet3p–GFP in the presence of either Ftr1p wild-type or Ftr1p(Δ361) demonstrates the latter's competence in 'chaperoning' Fet3–GFP to the plasma membrane. In contrast, note the strong perinuclear and weak plasma membrane localization of Fet3p–GFP when this fluorescent fusion is produced in the absence of any Ftr1p protein. For (**B**) and (**D**), several of the Ftr1p mutant proteins were produced in plasmid p703FTR1–YFP. (**B**) p703FTR1–YFP plasmids, as indicated, were transformed into strain 1457*ftr1Δ* (left-hand and middle images). In the right-hand image, p703FTR1–YFP alone was transformed into strain 1457*fet3Δftr1Δ*. Note the plasma membrane localization of wild-type and mutant Ftr1p–YFP in the presence of Fet3p that is lacking when Ftr1p–YFP is produced in Fet3p's absence (right-hand image). In (**C**) and (**D**), mutant forms of p703FTR1–YFP (as indicated) were transformed into strain 1457*ftr1Δ*, and trafficking of these Ftr1–YFP proteins to the plasma membrane in the presence of endogenous Fet3p was assessed by confocal fluorescence microscopy. Note the wild-type localization of all mutants (compare with the left-hand image in **B**).

Finally, in addition to the above EXXE motifs, the C-terminal domain in Ftr1p contains the following amino acid sequence [C-terminal truncations examined (Δ344, Δ361, Δ364, Δ367, Δ369, and Δ379 respectively) are indicated by arrows]:

Δ344 Δ361 Δ364 Δ367 Δ369 Δ379

(↓)^{345}ELTEEQKRQLFAKMENI(↓)NFN(↓)EDG(↓)EI(↓)NVQENYELPE^{379}(↓)

The four EXXE motifs in this domain are underlined (the last two overlap). In contrast with the sharing of REXLE sequences as in Figures 4(A) and 4(B), none of the other fungal Ftr1p homologues contain a similar complement of EXXE sequences, although three do contain at least two such motifs [7]. We assessed the contribution that each of these several sequence elements made, if any, to iron uptake supported by Ftr1p.

Localization of a residue in the Ftr1p cytoplasmic domain required for wild-type iron-uptake activity

Stearman et al. [10] constructed an Ftr1p(Δ334) truncation and demonstrated that the iron uptake supported by this mutant protein was approx. 5% of the wild-type activity. The authors concluded that one or more of the EXXE motifs in this domain (as shown above) were critical to uptake function. We repeated their experiment with the Ftr1p(Δ334) protein, and with a somewhat less-severe truncation at Ftr1p(Δ344); both proteins exhibited an iron-uptake activity that was 5% of wild-type or less [Figure 5, Ftr1p species (1–344) and (1–334) respectively]. We have greatly extended such studies.

First we assessed the hypothesis suggested above that one or more of the C-terminal EXXE motifs were part of the iron-uptake pathway. Our approach was to serially substitute these glutamate residues and assess the iron-uptake activity of the various mutant proteins. The results of these mutagenesis experiments were completely negative: none of the site-directed E $\rightarrow$ A substitutions strongly affected iron uptake. All of these C-terminal domain EXXE mutants had at least 70% wild-type activity, with the majority of them not statistically different from wild-type. Note that the data in Figures 6 and 7 do not allow for precise quantification of Fet3p/Ftr1p protein (complexes) in the plasma membrane. They show only that the abundance of Ftr1p in the cell is reasonably independent of the Ftr1p species present (solution fluorescence) and that $>$90% of this protein is in the plasma membrane (confocal images, Figure 6). Conservatively, we assign

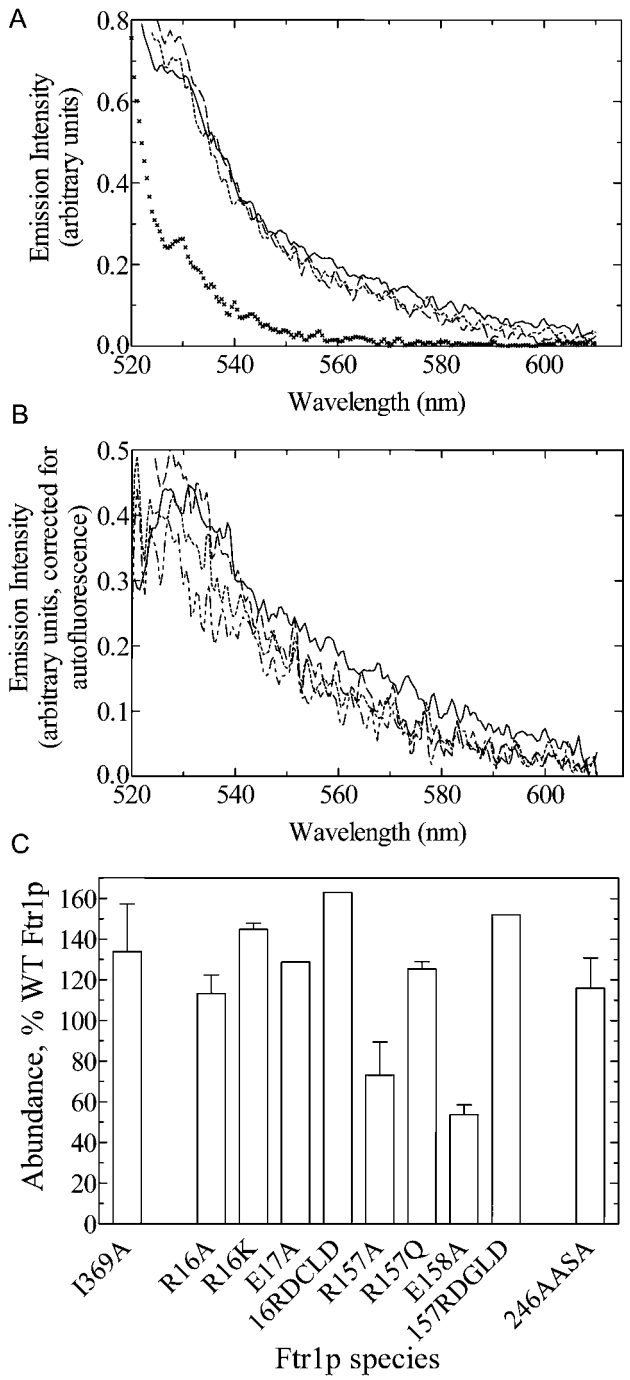

Figure 7 Quantification of Ftr1p mutant proteins by direct fluorescence

Strain 1457*ftr1Δ* was transformed with the wild-type and mutants of p703FTR1–YFP as indicated, and the transformants grown in synthetic medium in the presence of 500 μM ferrozine for 4 h. Cells were washed into FRET buffer at a cell density of 6×10^6 cells/ml. The fluorescence emission spectra of these suspensions were determined at an excitation of 510 nm on a PerkinElmer Model LS50B luminescence spectrometer. (**A**) Emission spectra of wild-type (solid line) and mutant forms of Ftr1p–YFP produced in strain 1457*ftr1Δ*. The mutants shown here are: Ftr1p(RDCLD)–YFP (short dashes) and Ftr1p(RDGLD)–YFP (long dashes). Note the spectra for strain 1457*ftr1Δ* producing non-fluorescent, wild-type Ftr1p from parental plasmid p703FTR1 (xxx). (**B**) Ftr1p–YFP-specific spectra obtained by subtraction of the cellular autofluorescence seen in strain 1457*ftr1Δ* producing non-fluorescent, wild-type Ftr1p. The Ftr1p–YFP species illustrated are: WT (solid line); RDCLD (short dashes); RDGLD (long dashes); and R157A (mixed dashes). (**C**) Quantification of the fluorescence envelopes due to various mutant forms of Ftr1p–YFP produced in strain 1457*ftr1Δ* presented as a percentage of the control wild-type Ftr1p–YFP. All envelopes were from five, signal-averaged scans; those values with error bars (means ± S.E.) were from three independent analyses.

some degree of loss-of-function to Ftr1p mutants only if they support 50 % or less of the wild-type iron-uptake rate.

This result indicated that the C-terminus contained some other structural element(s) that contributed to iron uptake. To localize this element, a simple deletion analysis was performed to complement the one started by Stearman et al. [10]. The sites of these truncations are indicated by arrows (↓) in the sequence above. The results of this analysis are shown in Figure 5, where the iron uptake supported by various truncated forms of Ftr1p is given as a percentage of the wild-type activity. This analysis shows that of the 95 % activity loss seen in the Ftr1p(Δ344) mutant, three-quarters of this loss occurred in the Ftr1p(Δ367) mutant and essentially all of it was seen in the Ftr1p(Δ361) protein. In fact the major fraction of this activity loss occurred upon deletion of Glu^{368}-Ile^{369} as indicated by the data for the 1–369 compared with 1–367 truncations. However, as noted, Ftr1p(Δ334) exhibited < 5 % of wild-type activity, indicating that additional sequence motifs necessary for full permease function could reside between residues 334 and 364 based on the truncation analysis presented here (Figure 5).

The basis of the loss-of-function exhibited by the Δ367 Ftr1p truncation (and also the more severe truncations) was explored in two ways. First, we considered the possibility that these truncated Ftr1p species did not traffic normally to the plasma membrane with Fet3p. This possibility was assessed by confirming the plasma-membrane localization of Fet3p–GFP that was co-produced along with wild-type Ftr1p or with the various Ftr1p truncations listed in Figure 5. Indeed, using confocal fluorescence microscopy, we were able to demonstrate that, for example, Ftr1p(Δ361) was as proficient in 'chaperoning' Fet3p–GFP to the plasma membrane as was wild-type Ftr1p (Figure 6A, compare first with second image). The fluorescence in the plasma membrane was not strongly different in the two transformants, indicating qualitatively that the limited iron uptake supported by Ftr1(Δ361) was an expression of a true loss-of-function and not a loss-of-abundance. In the absence of any Ftr1p species, as in the strain 1457*fet3Δftr1Δ* used in this experiment, when Fet3p–GFP alone is produced the fusion protein remains primarily perinuclear (Figure 6A, right-hand image).

We used directed mutagenesis to identify the motif or residue within the sequence 362–369 implicated in this loss-of-function. Two results indicated that a significant fraction of this loss was associated with Ile^{369} (see sequence above). Firstly, as noted, deletion of Glu^{368}-Ile^{369} resulted in the loss of 70 % iron uptake through Ftr1p. Secondly, the Ftr1p(I369A) mutant exhibited this same loss-of-function (Figure 5). When introduced into Ftr1p–YFP, the I369A mutation had no effect on the plasma membrane localization of the permease when observed directly *via* its fluorescent tag (Figure 6B, compare second with first image); therefore, this residue is not required for Ftr1p trafficking to the plasma membrane along with the Fet3p produced endogenously (in the strain used, 1457*ftr1Δ*). Ftr1p–YFP produced in the absence of Fet3p (using strain 1457*fet3Δftr1Δ*) remains in vesicular compartments adjacent to the yeast plasma membrane (Figure 6B, last image). The possible role(s) of Ile^{369} in the permease activity of Ftr1p will be discussed briefly below.

Two transmembrane REXLE motifs are essential to iron permeation in Ftr1p

Stearman et al. [10] demonstrated that both glutamate residues in the ^{157}REGLE^{161} motif in TM4 were essential to Ftr1p function, since E → A substitutions at either Glu^{158} or at Glu^{161} resulted in loss of iron-uptake activity. Therefore, we assessed the role of the ^{16}RECLE^{20} motif in TM1, the role of the arginine residues in

the motifs in both TM1 and TM4, and the potential synergism between the glutamate residues in both motifs in overall iron uptake. With regard to the first two objectives, the results were simple and clear. Firstly, E → A substitutions at either Glu^{17} or Glu^{20}, like those at either Glu^{158} or Glu^{161} [10], inactivated Ftr1p, indicating that the RECLE and REGLE motifs were equally important in Ftr1p iron-uptake function (the cysteine residue in the former motif was not essential; results not shown). Secondly, R → Q substitution at either Arg^{16} (in TM1) or Arg^{157} (in TM4) also inactivated Ftr1p in iron uptake. Alanine (and aspartate) mutants at these two arginine residues were inactive in iron uptake also. These data sets are not shown since iron uptake for all of these mutants was the same as for an *ftr1Δfet4Δ*-containing strain, that is, a strain with no saturable iron-uptake activities.

We generated all of the above point mutations (single and multiple) in Ftr1p–YFP. All of these fluorescent fusion proteins exhibited the same loss of iron-uptake function as did the non-fluorescent mutants and, in addition, localized to the plasma membrane in a wild-type manner. This general pattern is illustrated for four of these mutants in Figure 6(C). Also, we determined the solution fluorescence of live cells producing these various mutants constructed in Ftr1p–YFP so as to assess the relative abundance of the various Ftr1p mutant proteins examined [23]. The fluorescence spectra for wild-type Ftr1p–YFP and for two of these mutants are shown in Figure 7(A). The background cell autofluorescence is shown also, using the host strain for this control, 1457*ftr1Δ*, and producing wild-type Ftr1p from p703FTR1. In Figure 7(B), the spectra for the cells producing four YFP fusions, including wild-type, are corrected for this cell fluorescence. Fluorescence envelopes like these were then quantified for all mutants constructed in Ftr1p–YFP; examples of these areas are presented in Figure 7(C) as a percentage of the envelope area for wild-type Ftr1p–YFP. By this criterion these Ftr1p mutants, and all others described below, were produced in abundance that was approx. 50 to 150 % that of wild-type. Furthermore, the confocal images, as in Figure 6 (panels B–D), indicated that the Ftr1p–YFP protein quantified in each case by this direct (scanning) solution fluorescence was equivalently localized to the plasma membrane.

With this relative quantification of Ftr1p abundance in the plasma membrane, we could more precisely evaluate the roles that the four glutamate residues and the two arginine residues played in iron uptake through Ftr1p. The fact that both REXLE motifs were probably in transmembrane domains (see Figure 1), suggested that they contributed to the trafficking of Fe^{3+} across the membrane, perhaps as functional elements in a pore or channel. If this inference were correct then we thought it reasonable to propose that some geometric or distance constraints would be placed on such elements. For example, we predicted that single E → D substitutions would lead to some intermediate effects on iron-uptake activity. This proved to be the case.

Thus, we generated a family of single and double E → D mutants at residues 17, 20, 158 and 161, and determined the iron-uptake activity supported by each. These results, summarized in Figure 8, showed first that our prediction was correct overall and, secondly, demonstrated that functionally Ftr1p tolerated the loss of one -CH_2- group differentially with respect to the four residue positions. Thus E^{20} and E^{158} were apparently the least able to accommodate for the distance constraint associated with the E → D substitution, while aspartate residues at position 17 or 161 supported uptake that was approx. 40 % of wild-type. The activity of the double mutants also suggested these types of differential effects. For example, the activity of the E17D/E20D double mutant was not significantly different from the activity of the E20D single mutant. This pattern characterized the E17D/E158D and E20D/E161D mutants as well (results not shown). In contrast,

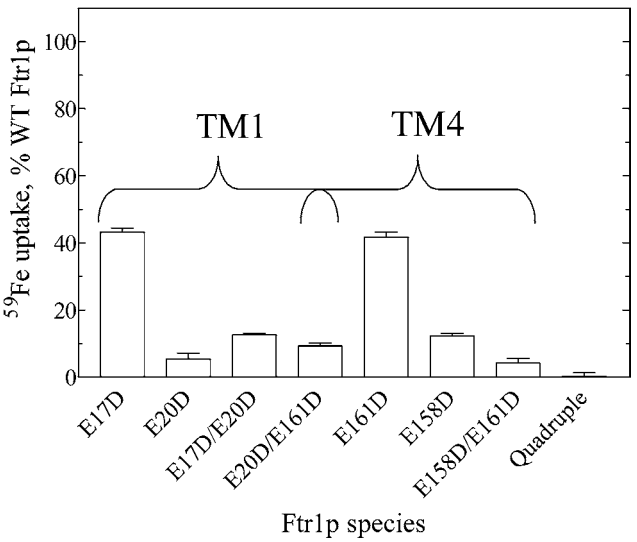

Figure 8 Structure–activity relationships in the Ftr1p REXLE motifs

^{59}Fe uptake assays were performed with strain 1457*ftr1Δ* transformed with wild-type and mutant forms of p703FTR1 as described in the legend for Figure 5.

the reduced activity of the E17D/E161D and E158D/E161D mutants suggested some additivity or synergy between these residues in their roles in iron permeation (Figure 8). The quadruple E → D mutant failed to support any detectable iron uptake, a result equivalent to that obtained with any one of the four E → A single mutants (or with either of the two R → A single mutants). With regard to the arginine residues that 'cap' the REXLE sequences in these two motifs, we surmised that R → K substitution might show a similar position dependence. Indeed, whereas the R157K mutant retained 60 % of wild-type uptake activity, the R16K mutant supported only 5 % of the ^{59}Fe uptake observed with the wild-type Fet3p/Ftr1p complex (results not shown).

A DASE motif in loop 6 and a glutamate in TM3 are involved in iron trafficking in Ftr1p

Another D/E motif, conserved in all fungal high-affinity iron permeases (Figure 4C), is DASE, designated here as loop 6 (Figure 1). Although D246A and E249A mutants supported wild-type iron uptake (indeed, they consistently exhibited enhanced activity), the D246Q/E249Q double mutant exhibited an uptake activity that was only slightly above the negative control (Figure 9). The D246A/E249A mutant was slightly more active than this with an activity that was 12 % of wild-type. In contrast, a 'residue-switch' D246E/E249D mutant was fully wild-type in uptake activity. All of these loop 6 mutant proteins were trafficked normally to the plasma membrane and were produced in normal abundance by the criteria exemplified in Figures 6 and 7. The trafficking of the ^{246}AASA^{249} double mutant in Ftr1p–YFP is shown in Figure 6(D) as an example of this. These results indicate that Asp^{246} and Glu^{249} function together in support of iron trafficking in the Fet3p/Ftr1p complex in a fashion that involves the carboxylate side chain that each possesses.

Finally, the ^{85}EDXXE^{89} sequence at the interface between loop 2 (extracellular) and TM3 (Figure 1) was tested for iron-uptake function. Although Ftr1p(E85A/D86A) exhibited wild-type uptake activity, Ftr1p(E89A) had only 20 % of that activity. The topological model of Ftr1p in Figure 1 places this glutamate

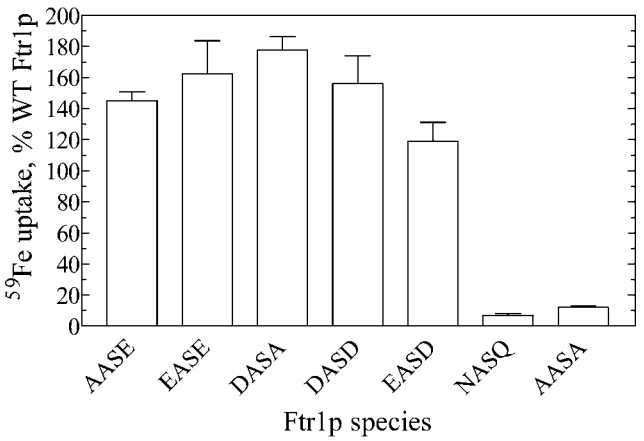

Figure 9 Structure–activity relationships in the Ftr1p loop 6 motif

^{59}Fe uptake assays were performed with strain 1457*ftr1Δ* transformed with wild-type and mutant forms of p703FTR1 as described in the legend for Figure 5. Error bars not evident are too small to be seen at this scale (means ± S.E.).

within TM3; if this is in fact the case then this residue could be a part of the glutamate-rich channel that includes the REXLE motifs above. Indeed, five of the eight fungal Ftr1p homologues listed in Figure 4 have an E(D/E)(I/L)WE sequence and topology model that places this conserved glutamate residue within the membrane as part of TM3.

DISCUSSION

The most intriguing functional characteristic of the Fet3p/Ftr1p high affinity iron-uptake complex is the coupling of ferroxidation catalysed by Fet3p with the iron uptake through Ftr1p. As emphasized in the Introduction, only iron that is the product of the Fet3p reaction, presumably Fe^{3+}, can be taken into the cell through Ftr1p. This type of product/substrate relationship is characteristic of metabolic channelling [17]. The objective of the work described here was to identify residues in Ftr1p that contributed to iron uptake overall and, by their location within the topological map of the protein, to infer where in this iron trafficking pathway they made their contribution to the overall process of 'chaperoning' the Fet3p-produced Fe^{3+} into the cell.

The results presented fully support the model of Ftr1p in the yeast plasma membrane shown in Figure 1. These data directly confirm the orientation of the C-terminus, and of four of the six proposed loop regions. However, the results do not strictly demonstrate that the $^{40}(HA)_2{}^{41}$ epitope is in a loop, but they are equally consistent with a model that has what we indicate as TM1 (residues 10–30, predicted) as part of a cytoplasmic N-terminal domain. This topology would have the N-terminus inside the cell, not outside as we suggest. However, the distribution of charged amino acids flanking the signal sequence that TM1 represents favours the N-terminal extracellar/C-terminal intracellular orientation shown in Figure 1. The first cytoplasmic loop in this model is strongly basic, conforming to the positive cytoplasmic 'rule' for signal-sequence orientation in the translocon [27–29]. Also, the model that we favour is similar to the one proposed for Fth1p, the vacuolar iron permease [16]. Given the strong homology among fungal iron permeases, the model in Figure 1 probably applies for all of these membrane proteins.

There are two well-characterized proteins that serve as examples of the types of sequence and structural motifs involved in the trafficking of Fe^{2+} and Fe^{3+}. These are ceruloplasmin and ferritin. Ceruloplasmin is a mammalian multicopper ferroxidase [13]. Crystallographic studies have identified two iron-binding sites that are approx. 7 Å apart (1Å ≡ 0.1 nm); in fact, a glutamic acid residue (residue 935 in human ceruloplasmin) may be part of the inner coordination sphere at both sites. Of the six residues implicated in these co-ordination spheres, three are glutamic acid and two are aspartic acid [30]. This concentration of acidic side chains is seen also at two different Fe^{2+} binding sites in mammalian ferritins. A DXXE motif lines the so-called 'three-fold channels' that connect the ferritin core to the outside surface of the H/L-chain heteropolymer. These two acidic residues are essential to the channelling of the Fe^{2+} into the core for its ferroxidation (or oxidation) concurrent with its core deposition [31]. H- and L-chains contain an additional, but not identical, glutamate-rich motif. In H-chains, a ^{62}EEREH^{66} sequence is a major part of the ferroxidase site that is unique to these chains. L-chains lack this sequence, but instead contain a sequence not found in H-chains, ^{53}REALE^{57}. These residues contribute to a mineralization site where Fe^{2+} is oxidized independent of ferroxidation [32]. It was this L-chain motif that Stearman et al. [10] recognized as a possible homologue of the REGLE one in TM4, thus suggesting the latter's importance in Ftr1p function.

A further example of the aspartic acid/glutamic acid-rich character of protein elements involved in iron binding, if not trafficking, is in the Fet4p protein in *S. cerevisiae* [20,33]. Fet4p supports low-affinity iron uptake ($K_m = 35\ \mu M$). The substrate for Fet4p is Fe^{2+}. Mutagenesis studies have targeted several residues in Fet4p that are likely to be in transmembrane domains in this protein. Alanine substitutions at Asp^{354}, Asp^{400} and Asp^{406} inactivate Fet4p in iron uptake. Based on a topology model of the protein, these three residues could form a cluster near the cytoplasmic end of the channel through which the Fe^{2+} passes into the cytosol [20].

In this context the multiple EXXE motifs in Ftr1p were natural candidates for ligands to Fe^{3+} in the trafficking and permeation processes [10]. As noted above, all of the fungal Ftr1p homologues possess two REXLE motifs, and both are most likely to be in transmembrane domains [7]. Stearman et al. [10] first showed that the second of these, the ^{157}REGLE^{161} motif in TM4, was essential to iron uptake. We have shown that the first of them, the ^{16}RECLE^{20} motif in TM1, plays an equally essential role. All four glutamate residues are required since all four E → A single mutants are inactive.

Our topology model places these two motifs near the midpoint of their respective transmembrane helices; thus, if the seven predicted transmembrane domains form a helical bundle, the RECLE and REGLE sequences could be aligned as illustrated in Figure 10. Given the orientation of helix 1 compared with helix 4, the two motifs would represent an 'inverted repeat' with the two arginine residues 'capping' a cluster of the four glutamic acid residues. Our results demonstrate that the two arginine residues play an equally essential role in the iron permeation process, suggesting that this inverted repeat represents a specific structure–function unit.

In this regard our results differ from those of Fang and Wang [34] who concluded that the ^{15}RESLE^{19} motif in the gene product of the *FTR1* gene from *C. albicans* was not essential. As in all of the Ftr1p homologues, CaFtr1p has two REXLE motifs; the second one is ^{157}REGLE^{161}, identical in sequence and sequence position to the one found in Ftr1p from *S. cerevisiae*. Although E → A substitutions in this latter motif, as well as an R → A substitution, inactivated CaFtr1p in iron uptake, the CaFtr1p (E16A) mutant is reported to have wild-type activity [34]. The fact that substitution of any one of the three essential residues found in this motif type, i.e. arginine and the two glutamic acid residues

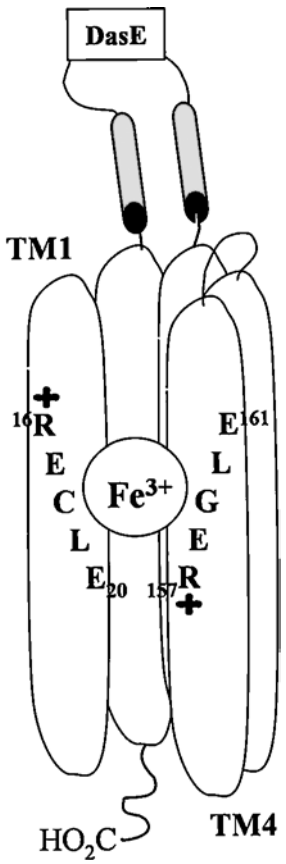

Figure 10 Schematic diagram depicting the iron 'channel' in Ftr1p

The cylinders represent Ftr1p transmembrane domains. Domains 2 and 3 have been omitted to reveal the REXLE motifs in domains 1 and 4. The DASE element in extracellular loop 6 is illustrated also. This diagram is based on the assumption that the seven transmembrane helices predicted for Ftr1p assemble into a barrel-like tertiary fold, forming an iron permeation channel through the membrane. The E residues could chelate the Fe^{3+} in this channel. The role of the essential R residues is not known. The spatial apposition of R and E residues in this putative 'inverted repeat' suggests that their electrostatic interaction might serve to 'gate' iron transport.

in the ^{16}RECLE^{20} element, inactivates ScFtr1p in iron uptake (the same result obtained if these individual mutations are made in the ^{157}REGLE^{161} element), indicates that both motifs are essential. It would seem unlikely that structure–function relationships in CaFtr1p are truly different in this regard.

Another example of this close homology between ScFtr1p and the two *Candida* iron permeases is the identical EDLWE motif at the interface between predicted extracellular loop 2 and TM3 (^{85}EDLWE^{89} in Figure 1). Glu^{89} in ScFtr1p is required for wild-type iron permeation activity, as indicated by the 80% loss of this activity in the Ftr1p(E89A) mutant. On the other hand, our mutagenesis experiments also showed that the first two acidic residues, i.e. Glu^{85}-Asp^{86}, were not essential to uptake. This result is of some interest since the aspartate residue (or glutamate in one instance) is found in only five of the eight fungal permease sequences so far fully archived, whereas all eight possess the C-terminal (W/Y)E motif. The possible location of this latter motif within TM3 suggests that the carboxylate side chain of Glu^{89} could contribute to the Fe^{3+} trafficking function associated with the two REXLE motifs. The role of this glutamate in the iron-uptake activity of the *Candida* Ftr1p homologues has not been investigated [34].

As noted, the Ftr1p sequence contains several other instances of closely repeated acidic residues, again, most often, glutamic acid. Each of the putative loop regions in Ftr1p contain these D/E elements (including, in part, the EDLWE above), but the only other one that appears to be involved in iron trafficking in the Fet3p/Ftr1p complex is the sequence ^{246}DASE^{249} in loop 6 that our topological model places in the extracellular space (Figures 1 and 10). The multicopper oxidase, ferroxidase domain in Fet3p is in this same space. Based on this shared orientation, we propose that the DASE motif, conserved in all fungal iron permeases (see Figure 4C), functions 'early' in the iron trafficking that couples the production of Fe^{3+} by Fet3p to the iron permeation due to Ftr1p. Our data cannot distinguish between possible roles that this motif might play in this process, e.g. as ligand to Fe^{3+} or in maintaining a specific protein conformation (these are not mutually exclusive possibilities). The fact that a relatively conservative substitution of carboxylate to carboxamido at the two acidic residues in this motif inactivated the permease, indicates that this motif could play a 'catalytic' rather than a 'structural' role in iron trafficking in this complex. Detailed kinetic analyses of iron uptake are underway to test the hypothesis that Fet3p-generated Fe^{3+} is channelled to the DASE motif without equilibration with bulk solvent.

Lastly, our results provide a caution that the sequence EXXE cannot simply be taken as a probable iron-binding motif. Naturally, the multiple EXXE motifs in the C-terminal domain of Ftr1p were brought to the attention of Stearman et al. [10] when they determined that a truncated Ftr1(Δ334) protein was inactive in iron uptake. However, our data show that the essential role that the C-terminus plays in Ftr1p function is not highly dependent on any of these glutamate residues. This domain, i.e. residues 335–404, is also not essential for the correct targeting to the plasma membrane. However, our further truncation and mutagenesis results have localized a sequence in the C-terminus that is required for function and, within that sequence, have shown that Ile^{369} plays a major role in iron uptake through Ftr1p.

What this role is remains unexplored; however, the residue type does suggest that this role could involve a protein–protein interaction stabilized by the burial of this non-polar side chain. Our data show that this putative interaction does not contribute to the association with Fet3p required for membrane targeting; however, they do not exclude the possibility that other such interactions between the two proteins modulate iron permeation. Possibly the active Fet3p/Ftr1p complex involves homo-oligomerization of one or both proteins, with Ile^{369} essential to an Ftr1p–Ftr1p interaction. An example of a metal ion permease homodimer is the Ctr1p high-affinity copper permease. In this case, the interaction domain is in the N-termini of the polypeptide chains [35]. We are currently examining the interactions between ferroxidase/permease pairs from *S. cerevisiae* (Fet3p and Fet5p, and Ftr1p and Fth1p) with the objective of delineating the interacting structural elements in each protein that support wild-type localization and uptake activities. This study should help to elucidate the role of Ile^{369} in the latter process.

We thank Ms Annette Romeo who constructed the 1457*fet3*Δ*ftr1*Δ and 1457*fet4*Δ*ftr1*Δ strains. The authors also acknowledge the extensive help given by Dr Wade Sigurdson in obtaining the confocal fluorescence images shown here. This research was supported by a grant to D. J. K. (DK53820) from the National Institutes of Health, Bethesda, MD, U.S.A.

REFERENCES

1 Askwith, C., Eide, D., Van Ho, A., Bernard, P. S., Li, L., Davis-Kaplan, S., Sipe, D. M. and Kaplan, J. (1994) The *FET3* gene of *S. cerevisiae* encodes a multicopper oxidase required for ferrous iron uptake. Cell (Cambridge, Mass.) **76**, 403–410

2 Askwith, C. and Kaplan, J. (1997) An oxidase-permease-based iron transport system in *Schizosaccharomyces pombe* and its expression in *Saccharomyces cerevisiae*. J. Biol. Chem. **272**, 401–405
3 de Silva, D. M., Askwith, C. C., Eide, D. and Kaplan, J. (1995) The *FET3* gene product required for high affinity iron transport in yeast is a cell surface ferroxidase. J. Biol. Chem. **270**, 1098–1101
4 Eck, R., Hundt, S., Härtl, A., Roemer, E. and Künkel, W. (1999) A multicopper oxidase gene from *Candida albicans*: cloning, characterization and disruption. Microbiology **145**, 2415–2422
5 Hassett, R. F., Yuan, D. S. and Kosman, D. J. (1998) Spectral and kinetic properties of the Fet3 protein from *Saccharomyces cerevisiae*, a multinuclear copper ferroxidase enzyme. J. Biol. Chem. **273**, 23274–23282
6 Knight, S. A., Lesuisse, E., Stearman, R., Klausner, R. D. and Dancis, A. (2002) Reductive iron uptake by *Candida albicans*: role of copper, iron and the *TUP*1 regulator. Microbiology **148**, 29–40
7 Kosman, D. J. (2003) The molecular mechanisms of iron uptake in fungi. Mol. Microbiol. **47**, 1185–1197
8 Morrissey, J. A., Williams, P. H. and Cashmore, A. M. (1996) *Candida albicans* has a cell-associated ferric-reductase activity which is regulated in response to levels of iron and copper. Microbiology **142**, 485–492
9 Ramanan, N. and Wang, Y. (2000) A high-affinity iron permease essential for *Candida albicans* virulence. Science (Washington, D.C.) **288**, 1062–1064
10 Stearman, R., Yuan, D. S., Yamaguchi-Iwai, Y., Klausner, R. D. and Dancis, A. (1996) A permease–oxidase complex involved in high-affinity iron uptake in yeast. Science (Washington, D.C.) **271**, 1552–1557
11 Frieden, E. and Osaki, S. (1974) Ferroxidases and ferrireductases: their role in iron metabolism. Adv. Exper. Med. Biol. **48**, 235–265
12 Dancis, A., Roman, D. G., Anderson, G. J., Hinnebusch, A. G. and Klausner, R. D. (1992) Ferric reductase of *Saccharomyces cerevisiae*: molecular characterization, role in iron uptake and transcriptional control by iron. Proc. Natl. Acad. Sci. U.S.A. **89**, 3869–3873
13 Solomon, E. I., Sundaram, U. M. and Machonkin, T. E. (1996) Multicopper oxidases and oxygenases. Chem. Rev. **96**, 2563–2605
14 Wang, T.-P., Quintanar, L., Severance, S., Solomon, E. I. and Kosman, D. J. (2003) Targeted suppression of the ferroxidase and iron trafficking activities of the multicopper oxidase, Fet3p, from *Saccharomyces cerevisiae*. J. Biol. Inorg. Chem. **8**, 611–620
15 Yuan, D. S., Dancis, A. and Klausner, R. D. (1997) Restriction of copper export in *Saccharomyces cerevisiae* to a late Golgi or post-Golgi compartment in the secretory pathway. J. Biol. Chem. **272**, 25787–25793
16 Urbanowski, J. L. and Piper, R. C. (1999) The iron transporter Fth1p forms a complex with the Fet5 iron oxidase and resides on the vacuolar membrane. J. Biol. Chem. **274**, 38061–38070
17 Anderson, K. S. (1999) Fundamental mechanisms of substrate channelling. Methods Enzymol. **308**, 111–145
18 Huffman, D. L. and O'Halloran, T. V. (2001) Function, structure, and mechanism of intracellular copper trafficking proteins. Annu. Rev. Biochem. **70**, 677–701
19 Rosenzweig, A. C. (2001) Copper delivery by metallochaperone proteins. Acc. Chem. Res. **34**, 119–128
20 Dix, D., Bridgham, J., Broderius, M. and Eide, D. (1997) Characterization of the FET4 protein of yeast. Evidence for a direct role in the transport of iron. J. Biol. Chem. **272**, 11770–11777
21 Sikorski, R. S. and Heiter, P. (1989) A system of shuttle vectors and yeast host strains designed for efficient manipulation of DNA in *Saccharomyces cerevisiae*. Genetics **122**, 19–27
22 Cormack, B. P., Bertram, G., Egerton, M., Gow, N. A., Falkow, S. and Brown, A. J. (1997) Yeast-enhanced green fluorescent protein (yEGFP), a reporter of gene expression in *Candida albicans*. Microbiology **143**, 303–311
23 Overton, M. C. and Blumer, K. J. (2002) Use of fluorescence resonance energy transfer to analyse oligomerization of G-protein-coupled receptors expressed in yeast. Methods **27**, 324–332
24 Hassett, R. and Kosman, D. J. (1995) Evidence for Cu(II) reduction as a component of copper uptake by *Saccharomyces cerevisiae*. J. Biol. Chem. **270**, 128–134
25 Drew, D., Sjostrand, d., Nilsson, J., Urbig, T., Chin, C., de Gier, J.-W. and von Heijne, G. (2002) Rapid topology mapping of *Escherichia coli* inner-membrane proteins by prediction and PhoA/GFP fusion analysis. Proc. Natl. Acad. Sci. U.S.A. **99**, 2690–2695
26 Nilssona, J., Perssona, B. and von Heijne, G. (2000) Consensus predictions of membrane protein topology. FEBS Lett. **486**, 267–269
27 Goder, V. and Spiess, M. (2003) Molecular mechanism of signal sequence orientation in the endoplasmic reticulum. EMBO J. **22**, 3645–3653
28 Hartmann, E., Rapoport, T. A. and Lodish, H. F. (1989) Predicting the orientation of eukaryotic membrane-spanning proteins. Proc. Natl. Acad. Sci. U.S.A. **86**, 5786–5790
29 von Heijne, G. (1986) The distribution of positively charged residues in bacterial inner membrane proteins correlates with the transmembrane topology. EMBO J. **5**, 3021–3027
30 Lindley, P., Card, G., Zaitseva, I., Zaitsev, V., Reinhammar, B., Selin-Lindgren, E. and Yoshida, K. (1997) An X-ray structural study of human ceruloplasmin in relation to ferroxidase activity. J. Biol. Inorg. Chem. **2**, 454–463
31 Treffry, A., Bauminger, E. R., Hechel, D., Hodson, N. W., Nowik, I., Yewdall, S. J. and Harrison, P. M. (1993) Defining the roles of the threefold channels in iron uptake, iron oxidation and iron-core formation in ferritin: a study aided by site-directed mutagenesis. Biochem. J. **296**, 721–728
32 Santambrogio, P., Levi, S., Cozzi, A., Corsi, B. and Arosio, P. (1996) Evidence that the specificity of iron incorporation into homopolymers of human ferritin L- and H-chains is conferred by the nucleation and ferroxidase centres. Biochem. J. **314**, 139–144
33 Dix, D. R., Bridgham, J. T., Broderius, M. A., Byersdorfer, C. A. and Eide, D. J. (1994) The *Fet4* gene encodes the low affinity Fe(II) transport protein of *Saccharomyces cerevisiae*. J. Biol. Chem. **269**, 26092–26099
34 Fang, H. M. and Wang, Y. (2002) Characterization of iron-binding motifs in *Candida albicans* high-affinity iron permease CaFtr1p by site-directed mutagenesis. Biochem. J. **368**, 641–647
35 Klomp, A. E., Juijn, J. A., van der Gun, L. T., van den Berg, I. E., Berger, R. and Klomp, L. W. (2003) The N-terminus of the human copper transporter 1 (hCTR1) is localized extracellularly, and interacts with itself. Biochem J. **370**, 881–889

Received 11 December 2003/11 February 2004; accepted 1 March 2004
Published as BJ Immediate Publication 1 March 2004, DOI 10.1042/BJ20031921